

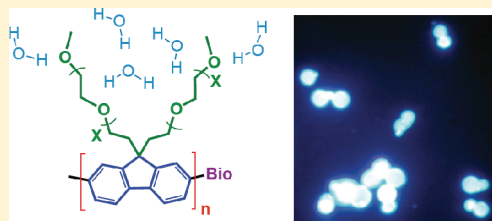
# Design and Synthesis of Monofunctionalized, Water-Soluble Conjugated Polymers for Biosensing and Imaging Applications

Christopher A. Traina, Ronald C. Bakus II, and Guillermo C. Bazan\*

Department of Materials and Chemistry and Biochemistry, Center for Polymers and Organic Solids, University of California, Santa Barbara, California 93106, United States

**S** Supporting Information

**ABSTRACT:** Water-soluble conjugated polymers with controlled molecular weight characteristics, absence of ionic groups, high emission quantum yields, and end groups capable of selective reactions of wide scope are desirable for improving their performance in various applications and, in particular, fluorescent biosensor schemes. The synthesis of such a structure is described herein. 2-Bromo-7-iodofluorene with octakis(ethylene glycol) monomethyl ether chains at the 9,9'-positions, i.e., compound **4**, was prepared as the reactive premonomer. A high-yielding synthesis of the organometallic initiator (dppe)Ni(Ph)Br (dppe = 1,2-bis(diphenylphosphino)ethane) was designed and implemented, and the resulting product was characterized by single-crystal X-ray diffraction techniques. Polymerization of **4** by (dppe)Ni(Ph)Br can be carried out in less than 30 s, affording excellent control over the average molecular weight and polydispersity of the product. Quenching of the polymerization with [2-(trimethylsilyl)ethynyl]magnesium bromide yields silylacetylene-terminated water-soluble poly(fluorene) with a photoluminescence quantum efficiency of 80%. Desilylation, followed by copper-catalyzed azide–alkyne cycloaddition reaction, yields a straightforward route to introduce a wide range of specific end group functionalities. Biotin was used as an example. The resulting biotinylated conjugated polymer binds to streptavidin and acts as a light-harvesting chromophore to optically amplify the emission of Alexa Fluor-488 chromophores bound onto the streptavidin. Furthermore, the biotin end group makes it possible to bind the polymer onto streptavidin-functionalized cross-linked agarose beads and thereby incorporate a large number of optically active segments.



## INTRODUCTION

Conjugated polymers offer a set of optoelectronic and light-harvesting properties that are unique for macromolecular materials and that are relevant for various emerging technologies.<sup>1–8</sup> For instance, thin films of these materials find applications in solution-processed field effect transistors,<sup>9</sup> polymer light-emitting diodes,<sup>10</sup> and plastic solar cells.<sup>11,12</sup> There is ample evidence that bulk behavior is influenced by the molecular characteristics of single chains, interchain relationships, and the processing history of the material.<sup>13–17</sup> Solvent interactions are important for determining the latter, and there is a significant body of work associated with the need to understand self-assembly in solution prior to film formation.<sup>18</sup>

Various conjugated polymer materials have also been studied as useful platforms for facilitating optically amplified chemical and biological fluorescent sensors.<sup>19–22</sup> The  $\pi$ -electron delocalization increases the electronic coupling between segments along the chain, thereby allowing excited states to interact with analytes within a larger sample volume, relative to small-molecule counterparts.<sup>23</sup> Environmental perturbations are therefore more easily detected. Solubility in aqueous media is a typical requirement for sensing biological targets. Conjugated polymers used for this purpose include pendant groups with ionic (i.e., conjugated polyelectrolytes)<sup>24–26</sup> or highly polar functionalities, for example, oligo(ethylene glycol) segments,<sup>27–30</sup> that compensate

for the hydrophobic nature of the backbone. Biosensors constructed from conjugated polyelectrolytes often rely on Coulombic interactions for binding to analytes or probe molecules.<sup>31,32</sup> While effective for binding to the desired substrate, these charges may also cause nonspecific binding to other species, potentially leading to increased background noise or false-positive readings.<sup>33,34</sup> Additionally, the sensitivity of these sensors can be compromised in certain environments, such as those containing high salt concentrations, as these ions can screen charges and disrupt sensor–target interactions.<sup>35</sup>

There are conjugated polymer-based biosensors that utilize covalently bound recognition probes for binding to analytes, such as the biotin-conjugated poly(phenyleneethynylene)s reported by Swager and co-workers.<sup>36</sup> The syntheses of such polymers often utilize step-growth procedures, whereby monomers with appended biotargeting molecules are copolymerized with those containing no biofunctionalization. Thus, the probes in these materials are distributed randomly along the backbone. Variability in sensing is reasonable under these circumstances, particularly when the statistical characteristics of the polymer chains are also taken into account.

**Received:** March 30, 2011

**Published:** July 13, 2011

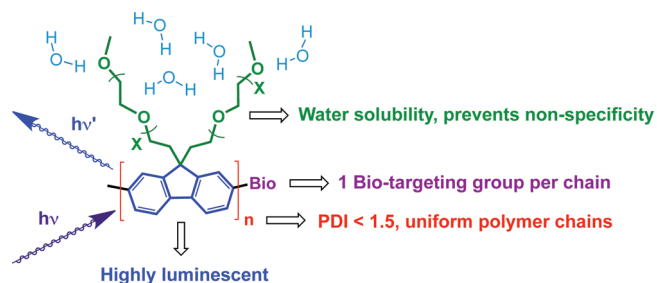


**Figure 1.** Structural and physical attributes of an ideal biosensing poly(fluorene) material.

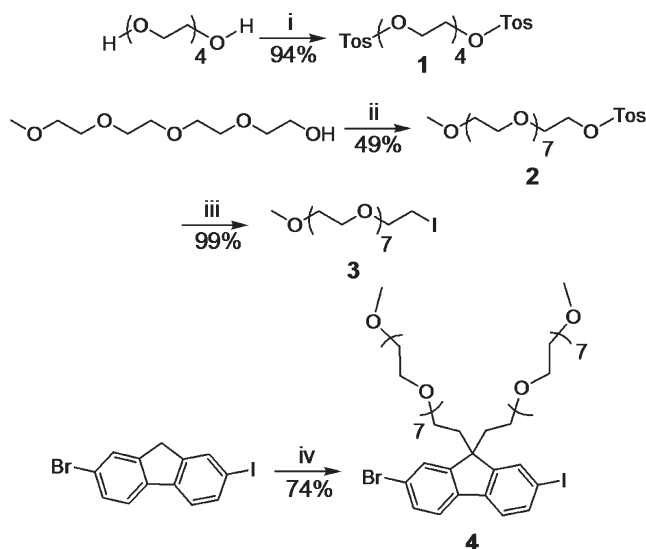
On the basis of the discussion above, one can envision several desirable properties of an ideal conjugated polymer for biosensor applications, namely, high photoluminescence quantum yield, water solubility, uniformity in chain length, resistance to nonspecific interactions, and a single site for biorecognition (Figure 1). To the best of our knowledge, such materials have not been reported and their preparation would require taking full advantage of modern polymer synthesis techniques. Current conjugated polymer syntheses generally involve Suzuki<sup>37</sup> or Stille<sup>38</sup> reaction schemes to couple a bis(halo)aryl species to an arylbisboronate or -bistannane, respectively, and under these conditions, high molecular weight polymers have been generated.<sup>39,40</sup> These step-growth polymerizations may suffer from lack of control, necessitating purification of the crude product; furthermore, significant variations in physical properties can occur between different batches of the same polymer.<sup>41,42</sup> As such, the wide scope of conjugated polymer biosensor applications can benefit from improved synthetic procedures.

In this paper we detail a general synthetic approach for accessing water-soluble conjugated polymers with excellent molecular weight uniformity and with chain end functionalization comprising reactive groups capable of selective postsynthesis modification reactions of wide scope. The work utilizes a well-defined, highly active transition-metal initiator for mediating controlled polymerization and demonstrates “click” chemistry protocols amenable for introduction of specific probes. As a final point, we show that the overall process allows biotin incorporation and that this terminal functionality has been shown to be reactive through solution and surface binding experiments to commercially available soluble streptavidin protein and streptavidin-conjugated microspheres, respectively.

## RESULTS AND DISCUSSION

**General Considerations for Monomer Design.** Chain growth methods have been developed that generate well-defined conjugated polymers for a limited number of systems.<sup>43</sup> For example, McCullough and co-workers<sup>44</sup> and Rieke and co-workers<sup>45</sup> reported polymerization of asymmetric monobromomonometallothiophene monomers by (L)NiCl<sub>2</sub> catalysts, where L is a bidentate bisphosphine ligand. One can thereby generate regioregular poly(3-alkylthiophenes) in good yield, with high degrees of polymerization (DP) and low polydispersity indices (PDIs < 1.4). The monohalomonometallo active monomer necessary for such polymerizations is generated in situ and can be achieved through metal–halogen exchange with a Grignard reagent.<sup>46</sup> This process is effective for 2,5-dibromo-3-alkylthiophene premonomers, requiring less than 1 h for full conversion to the active species. Fluorene-based polymers usually provide superior emission

## Scheme 1. Synthesis of Premonomer 4<sup>a</sup>

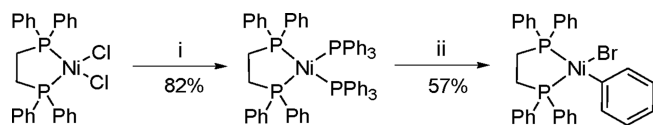


<sup>a</sup> Synthetic conditions: (i) tosyl chloride, triethylamine, ether, 0 °C to room temperature, 18 h; (ii) (a) NaH, THF, 2 h, (b) **1**, THF, 19 h; (iii) NaI, acetone, reflux, 15 h; (iv) (a) KH, THF, 1.5 h, (b) **3**, THF, 14 h.

characteristics over thiophene-based materials, especially in aqueous media, but metal–halogen exchange is slower for 2,7-dibromo-9,9'-dialkylfluorene systems, often requiring more than 8 h to form the active metalated species. Furthermore, this treatment can result in unreacted alkyl Grignard in solution or the generation of bismetalated fluorene species, both of which hinder chain growth characteristics.<sup>47</sup> In contrast, it has been shown that 2-bromo-7-iodofluorene premonomers subjected to similar conditions undergo metal–halogen exchange exclusively with iodide, generating the monometalated active species within 1 h.<sup>48</sup> Therefore, a 2-bromo-7-iodofluorene core was selected for our study.

Fluorene repeat units with oligo(ethylene glycol) side chains were targeted so to obtain water soluble polymers. The length of solubilizing oligo(ethylene glycol) group required some consideration: a chain which was too short would not provide the necessary solubility, whereas one that was too long would dilute the emissive component of the material and could potentially interfere with substrate binding. Fluorene-co-phenylene polymers containing alternating tris(ethylene glycol) monomethyl ether and tris(ethylene glycol) *tert*-butyl ester side chains show good organic solubility, but are not completely water-soluble.<sup>49</sup> 2-Bromo-7-iodofluorene with octakis(ethylene glycol) monomethyl ether chains at the 9,9'-positions was therefore selected. The octakis(ethylene glycol) chain was synthesized from two tetrakis(ethylene glycol) subunits,<sup>50</sup> as illustrated in Scheme 1. First, tosyl groups were installed on both ends of tetrakis(ethylene glycol) by treatment with tosyl chloride to give the bis(tosylate) **1**.<sup>51</sup> Tetrakis(ethylene glycol) monomethyl ether was then deprotonated with sodium hydride and slowly added to a THF solution of **1** to yield octakis(ethylene glycol) monomethyl ether tosylate, **2**.<sup>52</sup> Conversion of the terminal tosyl group to iodide gave **3**.<sup>53</sup> Treatment of 2-bromo-7-iodofluorene with potassium hydride in THF, followed by addition of **3**, afforded the premonomer **4** in good yield.

**Initiator Selection.** Grignard metathesis polymerizations of 3-alkylthiophenes often rely on complexes such as [1,3-bis-(diphenylphosphino)propane]nickel dichloride [(dppp)NiCl<sub>2</sub>]<sup>54,55</sup>

Scheme 2. Synthesis of the (dppe)Ni(Ph)Br Catalyst/Initiator<sup>a</sup>

<sup>a</sup> Synthetic conditions: (i) 2 equiv of ethylmagnesium bromide, 2 equiv of PPh<sub>3</sub>, diethyl ether, 2 h; (ii) bromobenzene, THF, 40 h.

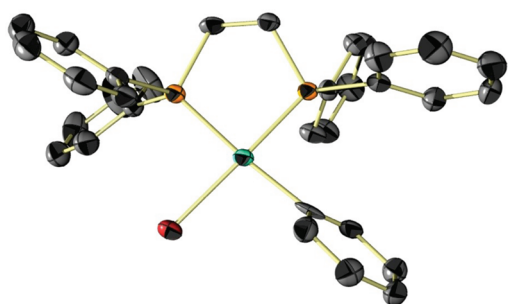


**Figure 2.** POV-Ray depiction of the molecular structure of (dppe)Ni(Ph)Br using 50% ellipsoids. Solvent and hydrogen atoms were omitted for clarity (C, gray; Br, red; Ni, green; P, orange).

or [1,2-bis(diphenylphosphino)ethane]nickel dichloride [(dppe)-NiCl<sub>2</sub>],<sup>56,57</sup> and it has been shown that each chain end of the polymer may be active for monomer addition.<sup>58</sup> End functionalization has been achieved by quenching of the polymerization with a suitable Grignard reagent (RMgX), generating MgX<sub>2</sub> and R-terminated polymer.<sup>59,60</sup> For systems catalyzed by (dppp)-NiCl<sub>2</sub>, double end functionalization is a possibility due to reaction at each terminus. Controlled 3-alkylthiophene polymerization and selective end functionalization have also been demonstrated using complexes of the type LNi(Ar)X, where L is a bidentate bisphosphine ligand, Ar is an aryl group, and X is a halogen.<sup>61–63</sup> For these reactions one chain end of the polymer corresponds to the Ar group. Initial screens in our laboratory demonstrated a faster activity with (dppe)NiCl<sub>2</sub>, relative to (dppp)NiCl<sub>2</sub>, for the polymerization of 2,5-dibromo-3-dodecylthiophene. For example, 120 s after monomer addition, (dppp)NiCl<sub>2</sub> yielded a polymer with a number average molecular weight (*M*<sub>n</sub>) of 14 000, while (dppe)NiCl<sub>2</sub> provided a product with *M*<sub>n</sub> = 21 000, as determined by gel permeation chromatography (GPC) relative to polystyrene standards.

On the basis of the preceding discussion, the complex *cis*-(bromo)(phenyl)[1,2-bis(diphenylphosphino)ethane]nickel, (dppe)Ni(Ph)Br in Scheme 2, was chosen as the initiator<sup>64</sup> and was synthesized in two steps from commercially available starting materials. First, a suspension of (dppe)NiCl<sub>2</sub> in the presence of PPh<sub>3</sub> was treated with 2 equiv of ethylmagnesium bromide to afford (dppe)Ni(PPh<sub>3</sub>)<sub>2</sub>. Oxidative addition of bromobenzene by (dppe)Ni(PPh<sub>3</sub>)<sub>2</sub> resulted in formation of the target, (dppe)Ni(Ph)Br. The structure of (dppe)Ni(Ph)Br was confirmed using <sup>1</sup>H, <sup>13</sup>C, and <sup>31</sup>P NMR spectroscopy, elemental analysis, and X-ray crystallography. Two doublets at 55 and 36 ppm are observed in the <sup>31</sup>P NMR spectrum, indicating two inequivalent phosphorus environments.<sup>62</sup> As shown in Figure 2, the solid-state structure as determined by single-crystal X-ray diffraction studies shows a pseudosquare planar geometry about

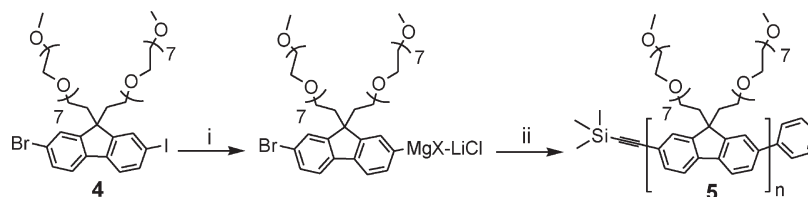
the nickel center and an out-of-plane twist of the ethyl backbone for the dppe ligand.

**Polymerization and End Functionalization.** Initial screens of the polymerization activity by using (dppe)Ni(Ph)Br were conducted with 2,5-dibromo-3-dodecylthiophene. A high degree of polymerization and low polydispersity were achieved (DP ≈ 100–200, PDI ≈ 1.1) with short reaction times (~5 min; see the Supporting Information), and a linear dependence of molecular weight could be demonstrated through adjustment of the initiator to monomer ratio. Complex (dppe)Ni(Ph)Br also proved similarly successful for polymerization of bis(alkoxy)phenyl and 9,9'-dialkylfluorene monomers (Supporting Information).

Subsequent studies focused on the polymerization of **4**, as shown in Scheme 3. Treatment of **4** with isopropylmagnesium chloride–lithium chloride complex at –35 °C for 40 min resulted in formation of the reactive species, which, in the presence of (dppe)Ni(Ph)Br, quickly polymerized (<30 s) to give the product as a yellow-green, waxy solid. Purification was achieved through selective precipitation and extraction procedures that took advantage of the high solubility of the product in solvents such as CH<sub>2</sub>Cl<sub>2</sub> and toluene, and its insolubility in hexane. With a monomer to catalyst ratio of 40:1, GPC analysis (DMF, 0.01% LiBr, calibrated against polystyrene standards) provided an *M*<sub>n</sub> in the 26 000–30 000 range with PDI values of 1.3–1.4. It is well-known that discrepancies can exist between the true molecular weight and that measured by GPC.<sup>65</sup> The polymer molecular weight was therefore measured by dynamic light scattering (DLS) techniques in DMF to obtain a value of 32 000, which is similar to that obtained by GPC. The number of repeat units can therefore be estimated using *M*<sub>n</sub> and the mass of each repeat unit (897 g/mol) to give a DP of between 29 and 33. Extension of the polymerization time beyond 30 s yielded only minimal gains in molecular weight at the expense of broader PDI values.

Quenching of polymerizations of **4** with [2-(trimethylsilyl)ethynyl]magnesium bromide was carried out to examine the efficiency of introducing a silylacetylene end group, as shown in Scheme 3. <sup>1</sup>H NMR analysis of the purified product revealed three resonances between 8.0 and 7.8 ppm, which correspond to the three unique aromatic proton environments.<sup>66</sup> Signals due to the methylene protons from the pendant oligo(ethylene glycol) chains appear between 3.6 and 2.6 ppm,<sup>67</sup> and the singlet attributed to the trimethylsilyl-protected ethynyl group appears at 0.28 ppm.<sup>68</sup> These data are consistent with the structure of the product **5** in Scheme 3. An estimate of end group incorporation was calculated to gauge the efficiency of this procedure. An *M*<sub>n</sub> = 29 000 polymer (as measured by GPC) should contain approximately 32 units. Each aromatic <sup>1</sup>H NMR resonance accounts for two protons on the repeat unit, and therefore, a polymer with 32 repeat units should give rise to an integrated value of 64 protons for each aromatic resonance. For 100% end group incorporation, the trimethylsilyl group should integrate for 9 H, and a ratio of (trimethylsilyl)ethynyl to each aromatic resonance of 9:64 or 0.14 should result. The <sup>1</sup>H NMR spectrum of **5** gives an integral ratio of 8:64 or 0.125 from resonances at 0.28 ppm ((trimethylsilyl)ethynyl end group) and 8.0 ppm (one set of backbone aromatic protons). Division of this experimental value by the theoretical maximum, as calculated above, reproducibly demonstrated 80–90% acetylene end group incorporation into the polymer. End group incorporation was further confirmed using MALDI-TOF mass spectrometric analysis of a low molecular weight oligomer, prepared similarly to the polymer



Scheme 3. Polymerization and End Functionalization of 4<sup>a</sup>

<sup>a</sup> Synthetic conditions: (i) *i*PrMgCl·LiCl, THF, −35 °C, 40 min; (ii) (a) (dppe)Ni(Ph)Br, room temperature, 20 s, (b) [2-(trimethylsilyl)ethynyl]magnesium bromide, THF, 1.5 h.

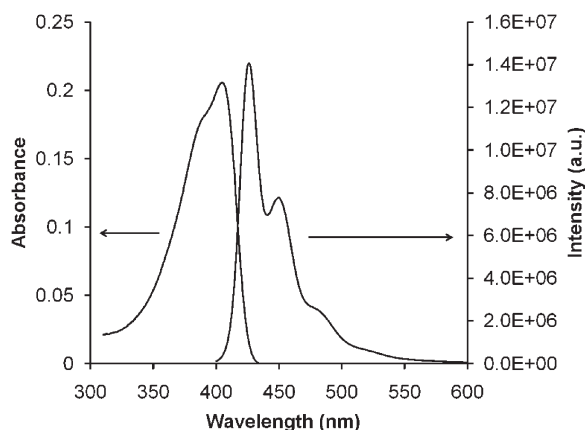


**Figure 3.** Absorption (left) and photoluminescence (right) spectra of polymer 5 in water.

but with a higher initiator:monomer ratio (Supporting Information). The resulting mass distribution exhibits peaks at 1968.0, 2864.4, and 3761.9 amu, corresponding to  $n = 2, 3$ , and 4 fluorene repeat units ( $MW = 896.51$ ), respectively, with phenyl and (trimethylsilyl)ethynyl end groups. These data confirm the presence of the desired end groups on the majority of product. Optimization studies showed that success of end group incorporation depends on the polymerization time and decreases if the terminating Grignard reagent is added more than 30 s after initiation. Therefore, care was taken to determine the optimal polymerization time (20 s) that achieved high molecular weight polymer while still retaining satisfactory end group incorporation.

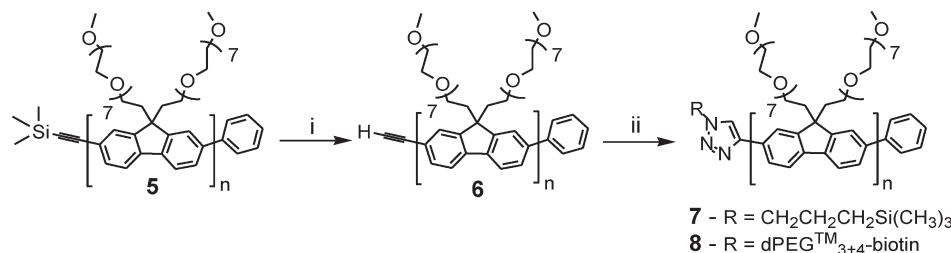
Polymer 5 is soluble in polar organic solvents, including  $\text{CH}_2\text{Cl}_2$ ,  $\text{CHCl}_3$ , methanol, ethanol, acetonitrile, and toluene. Furthermore, it can be dissolved in water and aqueous buffer solutions. Figure 3 shows the UV–vis absorption and emission properties in water, which are similar to those of other poly(fluorene)s.<sup>69</sup> Solutions of 5 display a broad absorption peak with a maximum ( $\lambda_{\text{max}}$ ) at 387 nm in  $\text{CHCl}_3$ , while the  $\lambda_{\text{max}}$  for aqueous solutions occurs at 405 nm, with a shoulder at 387 nm; the extinction coefficient is on the order of  $4 \times 10^4 \text{ M}^{-1} \text{ cm}^{-1}$ , as calculated per repeat unit. Solution-state photoluminescence measurements reveal a quantum yield of 0.8 in aqueous solution, which is comparable to those of other highly efficient water-soluble fluorene-based polymers.<sup>70,71</sup> Emission maxima are located at 420 nm in  $\text{CHCl}_3$  and 425 nm in water.

**End Group Functionalization via Click Chemistry.** The copper-catalyzed azide–alkyne cycloaddition reaction<sup>72</sup> is one type of click chemistry<sup>73</sup> that is useful for installing a wide variety of functionalities to organic compounds bearing alkyne or azide

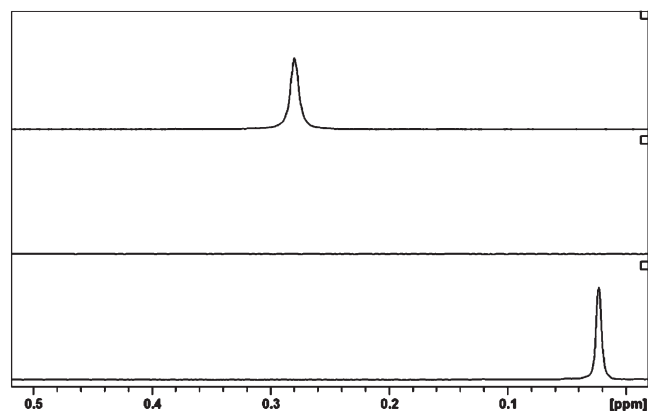
moieties.<sup>74</sup> Several biologically relevant organoazides are commercially available or can be readily synthesized; therefore, this reaction was a logical choice for attaching relevant functional probes. Typical reactions involve a terminal alkyne,<sup>75</sup> and thus, it was necessary to deprotect the terminal group of polymer 5. Desilylation of this alkyne can be accomplished by treatment of 5 with potassium carbonate in methanol,<sup>76</sup> as illustrated in Scheme 4, to yield the deprotected alkyne-bearing polymer 6. Figure 4 depicts a comparison of the upfield region (0.5–0 ppm) for the  $^1\text{H}$  NMR spectra of 5 and 6. It is evident that product 6 lacks the signal from the terminal trimethylsilyl protons, as was seen in the spectrum of 5; no differences in polymer solubility before and after desilylation were observed.

After deprotection, the terminal alkyne of 6 is active for click chemistry. To determine an approximate yield of this final step, polymer 6 was treated with a test reagent, (3-azidopropyl)trimethylsilane, in the presence of Cu(II)/sodium ascorbate in a THF/ $\text{H}_2\text{O}$ /*tert*-butyl alcohol solution<sup>77</sup> to give triazole-coupled product 7, as shown in Scheme 4. This test reagent was selected to provide a unique signal in the  $^1\text{H}$  NMR spectrum that can be used to determine reaction efficiency. Furthermore, GPC measurements of 5, 6, and 7 showed no major differences in  $M_n$  or PDI, indicating no change in the hydrodynamic volume of polymer due to potential undesirable side reactions. Therefore, a ratio was calculated between  $^1\text{H}$  NMR integrated intensities from the appended trimethylsilyl-containing test reagent and backbone aromatic proton resonances in 7. Polymers 5 and 7 each contain a terminal trimethylsilyl moiety, the former from initial in situ end functionalization and the latter from the final click reaction. The ratio of the integrated  $^1\text{H}$  NMR peak intensities between (trimethylsilyl)ethynyl and one set of backbone aromatic protons in 5 was compared to the ratio obtained for 7, and the values were found to be virtually identical (0.125 vs 0.120), indicating nearly quantitative conversion and successful postpolymerization incorporation of azide-containing organic reagents.

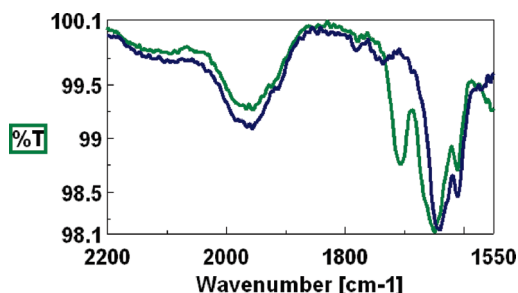
**End Group Conjugation for Biospecificity.** To demonstrate the applicability of this system to biosensing and imaging applications, it was necessary to attach an appropriate model reagent to the chain end, so as to provide a handle for studying probe–target specificity. For this purpose, we chose the biotin–streptavidin interaction, which is one of the strongest noncovalent interactions<sup>78</sup> and is often utilized as a model for biosensor applications<sup>79,80</sup> and as an affinity pair in standard bioassays.<sup>81,82</sup> Furthermore, derivatized streptavidin proteins and azide-containing biotin reagents are commercially available. As shown in Scheme 4, using a procedure similar to that for the preparation of 7, biotin-dPEG<sub>3+4</sub>-azide<sup>83</sup> (an azide-containing biotin with an oligo(ethylene glycol) spacer; see the Supporting Information for the full structure) was reacted with polymer 6, and the product, 8,

Scheme 4. Postpolymerization Click Conjugation of **5**<sup>a</sup>

<sup>a</sup> Synthetic conditions: (i) K<sub>2</sub>CO<sub>3</sub>, methanol, room temperature, 5 h; (ii) RN<sub>3</sub>, CuSO<sub>4</sub>·5H<sub>2</sub>O/sodium ascorbate, THF/*tert*-butyl alcohol/H<sub>2</sub>O, room temperature, 24 h. See the Supporting Information for the molecular structure of 8.

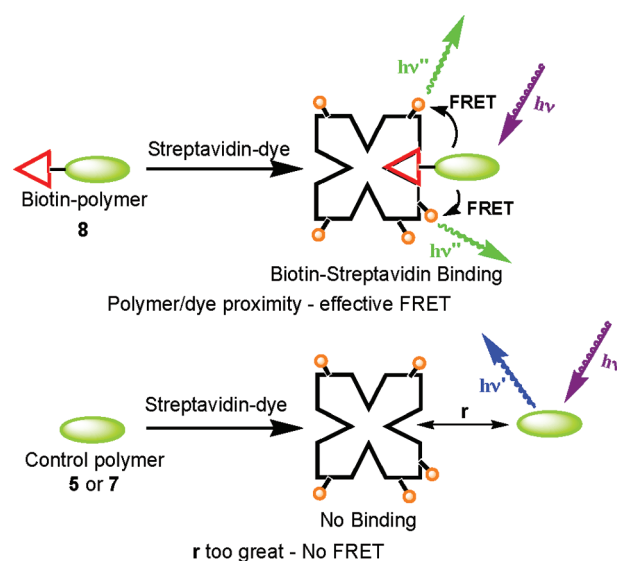


**Figure 4.** <sup>1</sup>H NMR spectra (0.5–0 ppm) of **5** (top), **6** (middle), and **7** (bottom), highlighting deprotection of the (trimethylsilyl)ethynyl end group of **5** (0.28 ppm) and subsequent click reaction of **6** with (3-azidopropyl)trimethylsilane to generate **7** (0.02 ppm).



**Figure 5.** Comparison of FT-IR spectra of **6** (blue) and **8** (green), highlighting new carbonyl bands (1708 and 1658 cm<sup>-1</sup>) in **8** from successful attachment of biotin reagent. The absence of the azide stretch (2100 cm<sup>-1</sup>) indicates efficient removal of the starting material.

was purified by dialysis against methanol. GPC analysis of **8** revealed no major differences in *M<sub>n</sub>* or PDI, relative to those of **5** or **6**. No resonances specific to the appended biotin moiety were observed in the <sup>1</sup>H NMR spectrum of **8**, likely due to overlap with polymer resonances, and therefore, NMR spectroscopy was unsuitable for determination of conjugation success. However, Fourier transform infrared (FT-IR) spectroscopy bands specific to the biotin fragment were useful in demonstrating attachment. As shown in Figure 5, the FT-IR spectrum of precursor polymer **6** contains bands near 1650 and 1600 cm<sup>-1</sup>; after the click reaction, new bands at 1710 and 1660 cm<sup>-1</sup> are observed, which

Scheme 5. Schematic for FRET Detection of Binding between **8** and Streptavidin–Alexa Fluor-488

are assigned to carbonyl signals from biotin<sup>84</sup> and amide groups in the linker. Additionally, no azide stretch was evident at 2100 cm<sup>-1</sup>, verifying removal of all unbound biotin reagent.

The ability of the biotin-functionalized polymer terminus of **8** to bind to a streptavidin receptor was used as a model assay to determine specific probe–analyte interactions. Streptavidin conjugates with appended chromophores are commercially available and were used to establish binding through fluorescence resonance energy transfer (FRET) experiments. FRET is a nonradiative transfer of energy from a donor absorbing moiety to an acceptor fluorophore.<sup>85</sup> A typical experiment involves excitation of a donor, followed by energy transfer to and emission by the acceptor, resulting in donor emission quenching and sensitization of acceptor luminescence. The efficiency of energy transfer is related to the spectral overlap between the donor and acceptor but, more importantly for the purpose of our experiments, is dependent on the spatial distance between the two and, thus, is useful for verification of binding interactions.<sup>86,87</sup> Typical effective FRET distances range between 1 and 10 nm, as energy transfer efficiency decays as 1/*r*<sup>6</sup>, with *r* being the distance between donor and acceptor.<sup>88</sup> A streptavidin reagent with appended Alexa Fluor-488 organic dye molecules (5 mol of dye/mol of streptavidin) was selected as the binding partner due

to suitable overlap between the emission of **8** and the absorption of the dye ( $\lambda_{\text{max,abs}} = 495 \text{ nm}$ ,  $\lambda_{\text{max,em}} = 520 \text{ nm}$ ). Binding between streptavidin and the terminal biotin of **8** should bring the optical partners into close proximity, resulting in efficient FRET. The overall process is illustrated in Scheme 5. In contrast, no interaction should exist between a control polymer (**5** or **7**) and streptavidin.

Thus, a solution of **8** (172 nM, calculated in terms of polymer chains on the basis of the  $M_n$  from GPC) in Tris buffer was treated with aliquots of the streptavidin–Alexa Fluor-488 dye conjugate (8.6 nM, calculated per protein molecule). As shown in Figure 6, before streptavidin–dye addition, excitation at 405 nm gave a typical polymer emission spectrum with a maximum near 425 nm. After introduction of one aliquot of streptavidin–dye, reduced polymer emission was observed with concomitant appearance of dye emission at 520 nm. The solution was treated with another aliquot of streptavidin–dye, and further attenuated polymer emission and dye luminescence enhancement can be observed. This process, shown in Figure 6, was repeated until no further decrease in polymer luminescence or increase in dye emission was detected, and the solution concentration of streptavidin–dye was noted (34.4 nM). It is known that streptavidin is a tetrameric protein capable of binding up to four biotin molecules,<sup>89</sup> and thus, the concentration of

biotin-binding sites should be equal to 4 times that of streptavidin protein molecules. The saturation concentration of streptavidin for this experiment, after which no further FRET was observed, therefore corresponds to an equivalent biotin-binding site concentration of 138 nM (i.e.,  $34.4 \text{ nM} \times 4$ ).<sup>90</sup> A comparison of this biotin-binding site concentration relative to the concentration of polymer chains in solution (172 nM) gives a ratio of  $\sim 0.8$ . As noted earlier, GPC data and  $^1\text{H}$  NMR spectra of **5** are consistent with approximately 80–90% (trimethylsilyl)ethynyl end group incorporation. Comparison between the NMR spectra of **5** and **7** indicates nearly quantitative click reactivity of this terminal alkyne, and therefore, approximately 80–90% of the polymer chains of **8** should contain a biotin end group. Thus, the ratio of streptavidin-bound polymer calculated from the FRET experiment (0.8) is approximately equal to the ratio of biotin-terminated polymer estimated from  $^1\text{H}$  NMR spectroscopy and GPC data (0.8–0.9), indicating excellent end group binding activity. An appropriate control experiment was performed using a polymer which contained no biotin terminus, **5** or **7** (Scheme 5). As anticipated, addition of streptavidin–dye to a solution of **5** or **7** gave rise to no significant polymer emission quenching or dye luminescence upon excitation at 405 nm (Supporting Information). The absence of energy transfer between **5** or **7** and the streptavidin–dye conjugate highlights the resistance of these polymers to non-specific interactions.

It should also be noted that significant enhancement of the Alexa Fluor dye emission was observed upon streptavidin–**8** binding due to FRET sensitization, as compared to direct excitation at 495 nm. As shown in Figure 6, at the concentrations used for this experiment, excitation at the polymer absorption of 405 nm gives rise to a greater than 5-fold increase in dye emission intensity as compared to direct dye excitation. This type of signal enhancement has been observed in other conjugated polymer–organic dye systems due to the increased absorption cross-section provided by the polymer, coupled with efficient energy transfer.<sup>19,25,26,91,92</sup> As expected, no signal enhancement is evident for the control system, streptavidin–Alexa Fluor-488 and **5**.

**Surface Reactivity of Biotin-Functionalized Polymers.** Another type of test was devised to examine the surface binding reactivity<sup>93</sup> of the biotin terminus of polymer **8**. Streptavidin-functionalized cross-linked agarose beads were incubated with a solution of **8** (or **5**, as a control). Upon removal of nonbound polymer, beads treated with **8** were highly luminescent under UV excitation, whereas no luminescence was observed for samples treated with **5**. Confocal microscopy images of individual particles confirmed this observation. Beads treated with **8** or **5** were imaged under bright-field illumination and in luminescence

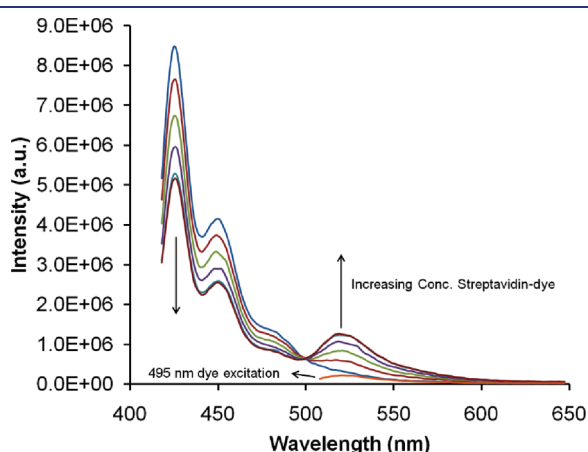


**Figure 6.** FRET from **8** (172 nM, excitation at 405 nm) to streptavidin–Alexa Fluor-488 (8.6 nM aliquots) showing decreased polymer emission (425 nm) and increased dye emission (520 nm) with increasing streptavidin–dye concentration. Saturation of dye emission was observed after addition of four aliquots (34.4 nM streptavidin–dye). The orange spectrum at the bottom corresponds to emission from direct dye excitation (495 nm) for the highest streptavidin–Alexa Fluor-488 concentration, highlighting signal enhancement due to FRET from **8**.

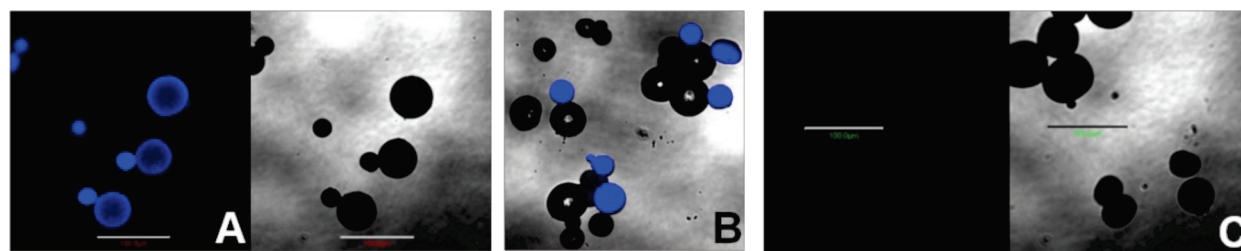


**Figure 7.** Confocal microscope images of streptavidin-coated beads treated with **8** (A) or **5** (C) captured in luminescence mode (left panel) or with bright-field illumination (right panel). The middle image (B) is an overlay of luminescence and bright-field images for a mixture of both sets of beads, showing emission from beads treated with **8**, but no emission is visible from beads treated with **5**. The scale bar corresponds to 100  $\mu\text{m}$ .



mode using 405 nm laser excitation. Figure 7A shows that beads treated with **8** exhibit blue emission. However, no luminescence was observed for those control particles treated with **5** (Figure 7C). Figure 7B displays the emission from a batch where emissive (treated with **8**) and nonemissive (treated with **5**) beads were mixed together. Thus, polymers such as **8** provide well-defined systems that are reactive for binding in solution and on surfaces and hold promise as luminescent reporters for a number of biological recognition applications.

## CONCLUSIONS

The work herein shows that it is possible to take advantage of monomer and catalyst design, together with appropriate termination reactions, for the synthesis of water-soluble monofunctionalized poly(fluorene)s with controlled molecular weight characteristics and excellent incorporation of protected ethynyl end groups. The organometallic initiator (dppe)Ni(Ph)Br allows polymerization reactions to be carried out in less than 30 s, yielding poly(fluorene)s with high  $M_n$  and low PDI values. Similar success in the preparation of other conjugated polymer structures is anticipated. After facile deprotection, the monofunctionalized poly(fluorene) reacts readily with azide-containing organic compounds in nearly quantitative yield, and this chemistry has been used to couple biorelevant targeting molecules to one of the polymer chain ends. This synthesis strategy results in highly luminescent materials, capable of engaging in biologically specific binding interactions. In one demonstration, a biorecognition event is monitored by the extent of energy transfer between a biotin-terminated poly(fluorene) and an organic dye-conjugated streptavidin. FRET between the polymer and dye due to biotin–streptavidin binding gives rise to decreased polymer luminescence and enhanced dye emission and scales with increased concentration of streptavidin–dye. Substantial signal enhancement upon polymer excitation was observed when compared to direct dye excitation. These materials are also active for surface binding; streptavidin-coated beads showed blue luminescence when treated with biotin-functionalized polymer, whereas no emission was evident in a control experiment. These solution and surface recognition capabilities make this material attractive as a component of luminescent bioassays or for in vitro tagging or imaging applications. More generally, a polymer, monofunctionalized with an alkyne moiety as demonstrated herein, is a versatile luminescent reagent platform which can be customized for a particular application by reaction with an appropriate azide starting material. Furthermore, this general scheme is also suitable for fluorene monomers with different substituents at the 9,9'-positions, for applications where a highly luminescent, well-defined, monofunctionalized material is important, but solubility in organic solvents may be more relevant.

## ASSOCIATED CONTENT

**S Supporting Information.** Synthesis and characterization of **1**, **2**, **3**, **4**, **5**, **6**, **7**, **8**, (dppe)Ni(PPh<sub>3</sub>)<sub>2</sub>, (dppe)Ni(Ph)Br, and (3-azidopropyl)trimethylsilane, graph of the control FRET experiment of **5** with streptavidin–Alexa Fluor-488, polymerization data for 2,5-dibromo-3-dodecylthiophene, 1-bromo-4-iodo-2,5-bis(octyloxy)benzene, and 2-bromo-7-iodo-9,9-dioctylfluorene by (dppe)Ni(Ph)Br, and crystallographic information for (dppe)Ni(PPh<sub>3</sub>)<sub>2</sub> and (dppe)Ni(Ph)Br. This material is available free of charge via the Internet at <http://pubs.acs.org>.

## AUTHOR INFORMATION

### Corresponding Author

bazan@chem.ucsb.edu

## ACKNOWLEDGMENT

Financial support from the Institute for Collaborative Biotechnologies, the National Science Foundation (Grant DMR 1035480), and the Department of Energy is gratefully acknowledged. We thank Alex Thomas for assistance with the confocal microscopy measurements.

## REFERENCES

- (1) Sun, S. S.; Dalton, L. R., Eds. *Introduction to Organic Electronic and Optoelectronic Materials and Devices*; CRC Press: Boca Raton, FL, 2008.
- (2) Delgado, J. L.; Bouit, P. A.; Filippone, S.; Herranz, M. A.; Martin, N. *Chem. Commun.* **2010**, 46, 4853–4865.
- (3) De Boer, B.; Facchetti, A. *Polym. Rev. (Philadelphia, PA, U.S.)* **2008**, 48, 423–431.
- (4) Pron, A.; Rannou, P. *Prog. Polym. Sci.* **2002**, 135–190.
- (5) Yamamoto, T. *Macromol. Rapid Commun.* **2002**, 23, 583–606.
- (6) Heeger, A. J. *Chem. Soc. Rev.* **2010**, 39, 2354–2371.
- (7) McQuade, D. T.; Pullen, A. E.; Swager, T. M. *Chem. Rev.* **2000**, 100, 2537–2574.
- (8) Bunz, U. H. F. *Macromol. Rapid Commun.* **2009**, 30, 772–805.
- (9) Facchetti, A. *Chem. Mater.* **2011**, 23, 733–758.
- (10) Grimsdale, A. C.; Chan, K. L.; Martin, R. E.; Jokisz, P. G.; Holmes, A. B. *Chem. Rev.* **2009**, 109, 897–1091.
- (11) Boudreault, P. L. T.; Najari, A.; Leclerc, M. *Chem. Mater.* **2011**, 23, 456–469.
- (12) Chen, J.; Cao, Y. *Acc. Chem. Res.* **2009**, 42, 1709–1718.
- (13) Chen, L. M.; Hong, Z.; Li, G.; Yang, Y. *Adv. Mater.* **2009**, 21, 1434–1449.
- (14) Schwartz, B. J. *Annu. Rev. Phys. Chem.* **2003**, 54, 141–172.
- (15) Virkar, A. A.; Mannsfeld, S.; Bao, Z.; Stingelin, N. *Adv. Mater.* **2010**, 22, 3857–3875.
- (16) Salles, A.; Kline, R. J.; DeLongchamp, D. M.; Chabinyc, M. L. *Adv. Mater.* **2010**, 22, 3812–3838.
- (17) Bazan, G. C. *J. Org. Chem.* **2007**, 72, 8615–8635.
- (18) van Bavel, S.; Veenstra, S.; Loos, J. *Macromol. Rapid Commun.* **2010**, 31, 1835–1845.
- (19) Thomas, S. W., III; Joly, G. D.; Swager, T. M. *Chem. Rev.* **2007**, 107, 1339–1386.
- (20) Herland, A.; Inganas, O. *Macromol. Rapid Commun.* **2007**, 28, 1703–1713.
- (21) Bazan, G. C.; Wang, S. *Springer Ser. Mater. Sci.* **2008**, 107, 1–37.
- (22) Miranda, O. R.; You, C. C.; Phillips, R.; Kim, I. B.; Ghosh, P. S.; Bunz, U. H. F.; Rotello, V. M. *J. Am. Chem. Soc.* **2007**, 129, 9856–9857.
- (23) Zhou, Q.; Swager, T. M. *J. Am. Chem. Soc.* **1995**, 117, 7017–7018.
- (24) Feng, F.; He, F.; An, L.; Wang, S.; Li, Y.; Zhu, D. *Adv. Mater.* **2008**, 20, 2959–2964.
- (25) Gaylord, B. S.; Heeger, A. J.; Bazan, G. C. *Proc. Natl. Acad. Sci. U.S.A.* **2002**, 99, 10954–10957.
- (26) Duarte, A.; Pu, K. Y.; Liu, B.; Bazan, G. C. *Chem. Mater.* **2011**, 23, 501–515.
- (27) Wosnick, J. H.; Mello, C. M.; Swager, T. M. *J. Am. Chem. Soc.* **2005**, 127, 3400–3405.
- (28) Xue, C.; Luo, F. T.; Liu, H. *Macromolecules* **2007**, 40, 6863–6870.
- (29) Kuroda, K.; Swager, T. M. *Chem. Commun.* **2003**, 26–27.
- (30) Phillips, R. L.; Kim, I. K.; Carson, B. E.; Tidbeck, B.; Bai, Y.; Lowary, T. L.; Tolbert, L. M.; Bunz, U. H. F. *Macromolecules* **2008**, 41, 7316–7320.

- (31) Liu, B.; Bazan, G. C. *J. Am. Chem. Soc.* **2004**, *126*, 1942–1943.
- (32) Liu, Y.; Ogawa, K.; Schanze, K. S. *J. Photochem. Photobiol., C* **2009**, *10*, 173–190.
- (33) Kim, I. B.; Dunkhorst, A.; Bunz, U. H. F. *Langmuir* **2005**, *21*, 7985–7989.
- (34) Dwight, S. J.; Gaylord, B. S.; Hong, J. W.; Bazan, G. C. *J. Am. Chem. Soc.* **2004**, *126*, 16850–16859.
- (35) Gaylord, B. S.; Heeger, A. J.; Bazan, G. C. *J. Am. Chem. Soc.* **2003**, *125*, 896–900.
- (36) Zheng, J.; Swager, T. M. *Chem. Commun.* **2004**, 2798–2799.
- (37) Sakamoto, J.; Rehahn, M.; Wegner, G.; Schluter, A. D. *Macromol. Rapid Commun.* **2009**, *30*, 653–687.
- (38) Carsten, B.; He, F.; Son, H. J.; Xu, T.; Yu, L. *Chem. Rev.* **2011**, *111*, 1493–1528.
- (39) Fu, Y.; Bo, Z. *Macromol. Rapid Commun.* **2005**, *26*, 1704–1710.
- (40) Coffin, R. C.; Peet, J.; Rogers, J.; Bazan, G. C. *Nat. Chem.* **2009**, *1*, 657–661.
- (41) Yokozawa, T.; Yokoyama, A. *Chem. Rev.* **2009**, *109*, 5595–5619.
- (42) Troshin, P. A.; Susarova, D. K.; Moskvina, Y. L.; Kuznetsov, I. E.; Ponomarenko, S. A.; Myshkovskaya, E. N.; Zakharcheva, K. A.; Balaki, A. A.; Babenko, S. D.; Razumov, V. F. *Adv. Mater.* **2010**, *20*, 4351–4357.
- (43) Miyakoshi, R.; Yokoyama, A.; Yokozawa, T. *J. Polym. Sci., Part A: Polym. Chem.* **2007**, *46*, 753–765.
- (44) McCullough, R. D.; Lowe, R. D. *J. Chem. Soc., Chem. Commun.* **1992**, *1*, 70–72.
- (45) Chen, T. A.; Rieke, R. D. *J. Am. Chem. Soc.* **1992**, *114*, 10087–10088.
- (46) Loewe, R. S.; Khersonsky, S. M.; McCullough, R. D. *Adv. Mater.* **1999**, *11*, 250–253.
- (47) Miyakoshi, R.; Yokoyama, A.; Yokozawa, T. *J. Am. Chem. Soc.* **2005**, *127*, 17542–17547.
- (48) Huang, L.; Wu, S.; Qu, Y.; Geng, Y.; Wang, F. *Macromolecules* **2008**, *41*, 8944–8947.
- (49) Wang, F.; Bazan, G. C. *J. Am. Chem. Soc.* **2006**, *128*, 15786–15792.
- (50) French, A. C.; Thompson, A. L.; Davis, B. G. *Angew. Chem., Int. Ed.* **2009**, *48*, 1248–1252.
- (51) Shao, M.; Dongare, P.; Dawe, L. N.; Thompson, D. W.; Zhao, Y. *Org. Lett.* **2010**, *12*, 3050–3053.
- (52) Wissner, A.; Kohler, C. A.; Goldstein, B. M. *J. Med. Chem.* **1986**, *29*, 1315–1319.
- (53) Grieco, P. A.; Parker, D. T. *J. Org. Chem.* **1988**, *53*, 3658–3662.
- (54) Osaka, I.; McCullough, R. D. *Acc. Chem. Res.* **2008**, *41*, 1202–1214.
- (55) Achord, B. C.; Rawlins, J. W. *Macromolecules* **2009**, *42*, 8634–8639.
- (56) Yokozawa, T.; Adachi, I.; Miyakoshi, R.; Yokoyama, A. *High Perform. Polym.* **2007**, *19*, 684–699.
- (57) Lanni, E. L.; McNeil, A. J. *J. Am. Chem. Soc.* **2009**, *131*, 16573–16579.
- (58) Tkachov, R.; Senkovskyy, V.; Komber, H.; Sommer, J. U.; Kiriya, A. *J. Am. Chem. Soc.* **2010**, *132*, 7803–7810.
- (59) Jeffries-EL, M.; Suave, G.; McCullough, R. D. *Adv. Mater.* **2004**, *16*, 1017–1019.
- (60) Javier, A. E.; Varshney, S. R.; McCullough, R. D. *Macromolecules* **2010**, *43*, 3233–3237.
- (61) Bronstein, H. A.; Luscombe, C. K. *J. Am. Chem. Soc.* **2009**, *131*, 12894–12895.
- (62) Senkovskyy, V.; Tkachov, R.; Beryozkina, T.; Komber, H.; Oertel, U.; Horecha, M.; Bocharova, V.; Stamm, M.; Gevorgyan, S. A.; Krebs, F. C.; Kiriya, A. *J. Am. Chem. Soc.* **2009**, *131*, 16445–16453.
- (63) Senkovskyy, V.; Sommer, M.; Tkachov, R.; Komber, H.; Huck, W. T. S.; Kiriya, A. *Macromolecules* **2010**, *43*, 10157–10161.
- (64) Amatore, C.; Jutand, A. *Organometallics* **1988**, *7*, 2203–2214.
- (65) Grell, M.; Bradley, D. D. C.; Long, X.; Chamberlain, T.; Inbasekaran, M.; Woo, E. P.; Soliman, M. *Acta Polym.* **1998**, *49*, 439–444.
- (66) Huang, F.; Zhang, Y.; Liu, M. S.; Jen, A. K. Y. *Adv. Funct. Mater.* **2009**, *19*, 2457–2466.
- (67) Pu, K. Y.; Fang, Z.; Liu, B. *Adv. Funct. Mater.* **2008**, *18*, 1321–1328.
- (68) Thomas, K. R. J.; Lin, J. T.; Lin, Y. Y.; Tsai, C.; Sun, S. S. *Organometallics* **2001**, *20*, 2262–2269.
- (69) Scherf, U.; List, E. J. W. *Adv. Mater.* **2002**, *14*, 477–487.
- (70) Zhu, B.; Han, Y.; Sun, M.; Bo, Z. *Macromolecules* **2007**, *40*, 4494–4500.
- (71) Qin, C.; Wu, X.; Gao, B.; Tong, H.; Wang, L. *Macromolecules* **2009**, *42*, 5427–5429.
- (72) Meldal, M.; Tornøe, C. W. *Chem. Rev.* **2008**, *108*, 2952–3015.
- (73) Kolb, H. C.; Finn, M. G.; Sharpless, K. B. *Angew. Chem., Int. Ed.* **2001**, *40*, 2004–2021.
- (74) Amblard, F.; Cho, J. H.; Schinazi, R. F. *Chem. Rev.* **2009**, *109*, 4207–4220.
- (75) Rostovtsev, V. V.; Green, L. G.; Fokin, V. V.; Sharpless, K. B. *Angew. Chem., Int. Ed.* **2002**, *41*, 2596–2599.
- (76) Maji, M. S.; Pfeifer, T.; Studer, A. *Chem.—Eur. J.* **2010**, *16*, 5872–5875.
- (77) Shi, W.; Dolai, S.; Averick, S.; Fernando, S. S.; Saltos, J. A.; L'Amoreaux, W.; Banerjee, P.; Raja, K. *Bioconjugate Chem.* **2009**, *20*, 1595–1601.
- (78) Green, N. M. *Methods Enzymol.* **1990**, *184*, 51–67.
- (79) Bernier, S.; Garreau, S.; Bera-Aberem, M.; Gravel, C.; Leclerc, M. *J. Am. Chem. Soc.* **2002**, *124*, 12463–12468.
- (80) Ji, E.; Wu, D.; Schanze, K. S. *Langmuir* **2010**, *26*, 14427–14429.
- (81) Wilchek, M.; Bayer, E. A. *Methods Enzymol.* **1990**, *184*, 5–13.
- (82) Wilchek, M.; Bayer, E. A. *Anal. Biochem.* **1988**, *171*, 1–32.
- (83) Obtained from Quanta Biodesign, <http://quantabiodesign.com>. (accessed November, 2010).
- (84) Lapin, N. A.; Chabal, Y. J. *J. Phys. Chem. B* **2009**, *25*, 8776–8783.
- (85) Forster, T. *Naturwissenschaften* **1946**, *33*, 166–175.
- (86) Huebsch, N. D.; Mooney, D. J. *Biomaterials* **2007**, *28*, 2424–2437.
- (87) Campbell, R. E. *Anal. Chem.* **2009**, *81*, 5972–5979.
- (88) Forster, T. *Discuss. Faraday Soc.* **1959**, *27*, 7–17.
- (89) Laintinen, O. H.; Nordlund, H. R.; Hytonen, V. P.; Kulomaa, M. S. *Trends Biotechnol.* **2007**, *25*, 269–277.
- (90) Hu, S.; Yang, H.; Cai, R.; Liu, Z.; Yang, X. *Talanta* **2009**, *80*, 454–458.
- (91) Liu, B.; Bazan, G. C. *J. Am. Chem. Soc.* **2006**, *128*, 1188–1196.
- (92) Wang, S.; Hong, J. W.; Bazan, G. C. *Org. Lett.* **2005**, *7*, 1907–1910.
- (93) Bayer, E. A.; Wilchek, M. *J. Chromatogr.* **1990**, *510*, 3–11.